Quaternary Science Reviews 250 (2020) 106654

Contents lists available at ScienceDirect

Quaternary Science Reviews

journal homepage: www.elsevier.com/locate/quascirev

Ocean-rafted pumice constrains postglacial relative sea-level and supports Holocene ice cap survival

W.R. Farnsworth [a, b, c, *], W. Blake Jr. [d], E.R. Guðmundsdóttir [a, c, e], Ó. Ingólfsson [e], M.H. Kalliokoski [a], G. Larsen [a, e], A.J. Newton [f], B.A. Óladóttir [e, g], A. Schomacker [c]

[a] Nordic Volcanological Center, University of Iceland, Sturlugata 7, Reykjavík, IS-101, Iceland
[b] Arctic Geology Department, University Centre in Svalbard (UNIS), N-9171, Longyearbyen, Norway
[c] Department of Geosciences, UiT The Arctic University of Norway, P.O. Box 6050, Langnes, N-9037, Norway
[d] Formerly with the Geological Survey of Canada, 601 Booth St., Ottawa, Canada
[e] Institute of Earth Sciences, University of Iceland, Sturlugata 7, Reykjavík, IS-101, Iceland
[f] School of GeoSciences, University of Edinburgh, Drummond St., Edinburgh, EH8 9XP, Scotland, UK
[g] IMO Icelandic Meteorological Office, Reykjavík, Bústaðavegur 7-9, IS-105, Iceland

ARTICLE INFO

Article history:
Received 17 August 2020
Received in revised form
9 October 2020
Accepted 11 October 2020
Available online xxx

Keywords:
Tephrochronology
Holocene thermal maximum
Iceland
Svalbard
Katla

ABSTRACT

Distally deposited tephra from explosive volcanic eruptions can be a powerful tool for precise dating and correlation of sedimentary archives and landforms. However, the morphostratigraphic and chronological potential of ocean-rafted pumice has been under-utilized considering its long observational history and widespread distribution on modern and palaeo-shorelines around the world. Here we analyze the geochemical composition and elevation data of 60 samples of ocean-rafted pumice collected since 1958 from raised beaches on Svalbard. Comparison of pumice data with postglacial relative sea-level history suggests eight distinct pumice rafting events throughout the North Atlantic during the Middle and Late Holocene. Analyzed ocean-rafted pumice exhibit consistent silicic composition characteristic of deposits from Iceland's volcanic system, Katla. Eruption-triggered jökulhlaups are key drivers of the transport of pumice from the Katla caldera to beyond the coast of Iceland and into the surface currents of the North Atlantic Ocean. Thus, the correlation of distinct, high-concentration pumice horizons from Katla deposited along raised Middle Holocene beach ridges in Svalbard further advocates for the persistence of the Mýrdalsjökull ice cap through the Holocene thermal maximum.

1. Introduction

The distal deposition of tephra in far-field locations resulting from explosive volcanism has revolutionized how we can correlate and precisely date sedimentary archives and landforms (e.g., Lowe 2011; Davies 2015). The application of tephra as a geochronological tool (Thórarinsson 1944) is unparalleled in spatial and temporal precision, providing the potential to investigate synchronicity or lag-response to climate forcings (Miller et al., 2012; Muschitiello et al., 2017). The number of studies of far travelled (crypto-) tephra have increased progressively over the last few decades (e.g., Davies 2015; Ponomareva et al., 2015; Timms et al., 2019; Abbott et al., 2020; Kalliokoski et al., 2020). However, geological investigations of ocean-rafted pumice have essentially been left adrift, except for a few laboratory investigations (Whitham and Sparks 1986), occurrence/archaeological case studies (Salvigsen 1984; Newton 2000, 2018; Romundset and Lakeman 2019), and dissertations (Binns 1971; Knape 1971; Newton 1999a). While the majority of Quaternary and volcanology tephra studies focus on primary deposits (e.g. Larsen 2000; Guðmundsdóttir et al., 2011; McCulloch 2017), investigations of ocean-rafted pumice exemplify the potential chronological and environmental value of tephra that has been reworked or transformed (i.e. cryoturbation; Kirkbride and Dugmore 2005; Dugmore et al., 2020). Furthermore, pumice rafting events have gained recent attention due to their ability to rapidly disperse marine organisms over long distances as well as their potential to replenish shallow marine and coastal ecosystems (Bryan et al. 2004, 2012; Carey et al., 2018). Developments in remote sensing and geophysical methods have allowed for near

* Corresponding author. Nordic Volcanological Center, University of Iceland, Sturlugata 7, IS-101, Iceland.
E-mail address: WesleyF@hi.is (W.R. Farnsworth).

https://doi.org/10.1016/j.quascirev.2020.106654

real-time identification of pumice rafts, as well as tracking of their dispersal trajectories (Jutzeler et al., 2020). Here we highlight how a multidisciplinary investigation of ocean-rafted pumice can enhance our understanding of postglacial relative sea-level as well as volcanic/ice cap conditions during eruptions. Major elemental geochemical analysis of 60 samples of ocean-rafted pumice collected from three distinct regions of Svalbard during three field campaigns (1958, 2015, and 2019) provides a framework of distally deposited pumice to the high Arctic during the Holocene. Pumice provides a morphostratigraphic constraint on relative sea level and potentially a chronostratigraphic constraint. Furthermore, geochemical investigations of pumice found in Svalbard strengthen evidence of one of Iceland's larger ice caps surviving through the Holocene thermal maximum. Ultimately this study utilizes a 60-year old archived collection of pumice as a reminder of its geochronological potential given modern process understanding and analytical techniques.

The term *pumice* describes low density (<1 g cm^{-3}), highly vesicular (up to 90%) volcanic glass-foam with compositions varying from basaltic, intermediate to silicic (Thórarinsson 1974; Fisher and Schmincke 1984; Whitham and Sparks 1986). Pumice can form both subaerially and in subaqueous or subglacial conditions (Kokelaar 1986; Cashman and Fiske, 1991). Experiments suggest the low density; vesicular particles can remain afloat in water for at least 18 months (Whitham and Sparks 1986) and drift around in ocean currents until ultimately sinking to the ocean floor (Binns 1971; Newton 1999a; Fang et al., 2019).

Due to the buoyant nature of pumice, it has a long history of observation and description from (raised) beaches throughout the North Atlantic with investigations from the British Isles, Scandinavia and Svalbard (Fig. 1; Balchin 1941; Undas 1942; Noe-Nygaard 1951; Feyling-Hanssen 1955; Binns 1971, 1972; Schytt et al., 1968; Blake 1970; Boulton and Rhodes 1974; Salvigsen 1978; 1981; 1984; Newton 1999a, 1999b; Romundset and Lakeman 2019). The first descriptions from Norway are from the mid-18th century (Strøm, 1762), while descriptions from Svalbard are noted by early expeditions of explorers and researchers through the last 200 years (Parry 1828; Nordenskiöld 1863; De Geer 1896). While early pumice observations focused on its occurrence and distribution, pumice horizons were first correlated with palaeo-shorelines across wider regions by Donner and West (1957), and were first related to radiocarbon-dated shorelines by Blake (1961a).

Donner and West (1957) initially mapped two horizons of pumice-rich shorelines across either side of the Hinlopen Strait in northern Svalbard (Fig. 1B). Further investigations highlighted three (Blake 1961a), four (Boulton and Rhodes 1974; Salvigsen 1984) and up to seven potential pumice horizons (Newton 1999a). Difficulties with precise correlations stemmed from low-resolution geochemical data, challenges with radiocarbon correction and calibration as well as heterogenic relative sea-level history between pumice sites (Blake 1961b, 1970; Salvigsen 1984; Newton 1999a). Svalbard's uppermost pumice horizon, radiocarbon dated to 6.5 ^{14}C ka BP (*c.* 7.5 cal ka BP), was also characterized by the most abundant interval of rafted pumice (Boulton and Rhodes 1974). In some locations, the pumice horizon is described to have concentrations exceeding 10 clasts per square meter or several hundred in a few meters distance along the beach (Blake 1961a; Salvigsen 1984).

Lacking robust geochemical investigation, most early pumice investigations logically looked to Iceland as the probable source of the widespread ocean-rafted pumice (Parry 1828; Nordenskiöld 1874; Bäckström 1890; Noe-Nygaard 1951; Binns 1967, 1971,

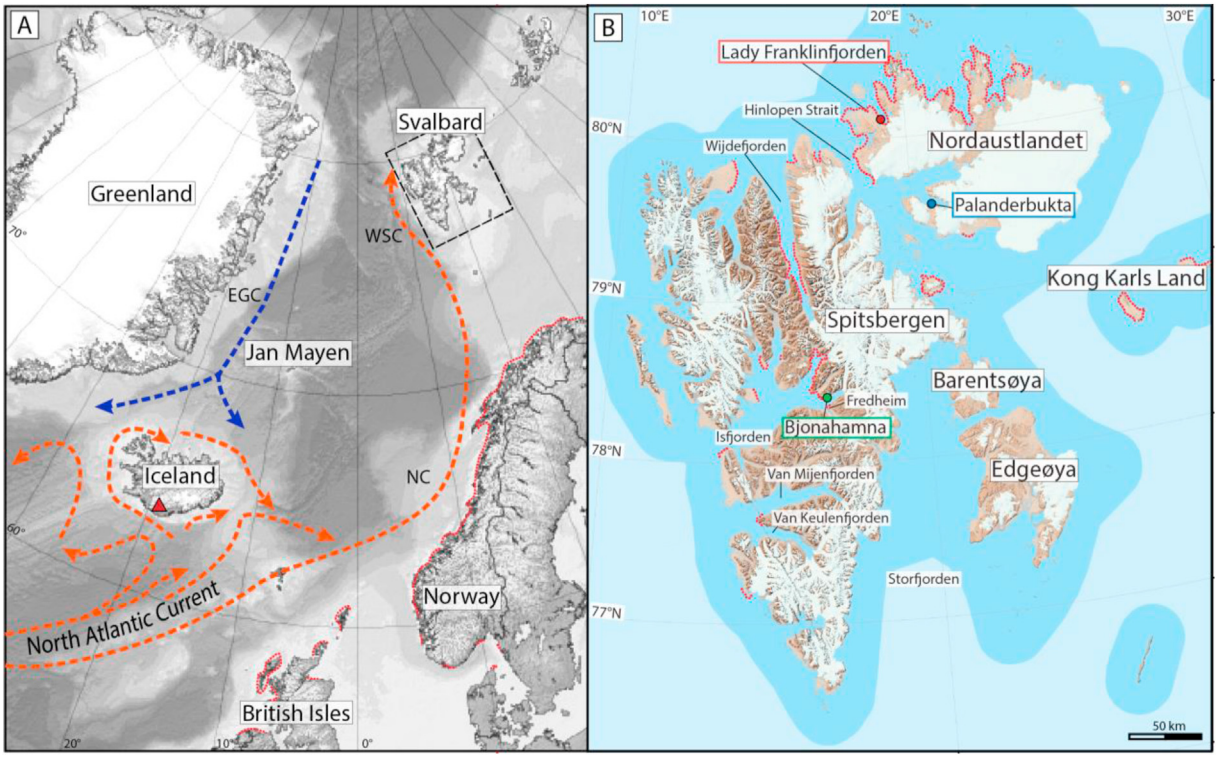

Fig. 1. Map of the North Atlantic region with major ocean and regional Icelandic surface currents indicated (warm currents in orange, cold currents in blue; Valdimarsson and Malmberg 1999). The North Atlantic Current transitions into the Norwegian Current (NC) and further into the West Spitsbergen Current (WSC). The East Greenlandic Current travels to the south (EGC). The Katla volcanic system is marked by a red triangle (Uwe Dedering under CC-BY-SA 3.0). B) Detailed map of Svalbard with major islands named and study sites indicated by colored circles (modified from TopoSvalbard © Norwegian Polar Institute 2020). Red dotted lines in both maps represent regions with described pumice modified from Newton (1999a). (For interpretation of the references to color in this figure legend, the reader is referred to the Web version of this article.)

1972; Peulvast and Dejou 1982; Salvigsen and Österholm 1982; Salvigsen 1984), while Boulton and Rhodes (1974) argued the rafted material originated from Jan Mayen based on trace element investigations. Noe-Nygaard (1951) argued the Hekla volcanic system to be the most likely source based on descriptions of rafts of pumice floating off the coast of Iceland following the 1947 eruption. However, Salvigsen (1984) argued Hekla to be an unlikely source of the North Atlantic's pumice due to its inland location, inferring pumice may have been derived from sea floor eruptions.

Newton (1999a) summarized previous works and detailed the distribution of pumice investigations in the North Atlantic. Furthermore, Newton (1999a) geochemically analyzed major elemental composition of pumice samples from Norway (n = 44; 6 sites), Iceland (n = 24; 6 sites) and Scotland (n = 50; 14 sites) which identified a prevalent and consistent dacitic geochemical signature. Comparison of major elemental composition data with earlier geochemical investigations was deemed challenging due to variable and low precision techniques (Blake 1970; Binns 1971, 1972; Boulton and Rhodes 1974; Newton 1999a). Based on geochemical comparisons to volcanic ash layers in Iceland, the majority of ocean rafted pumice in the North Atlantic geochemically correlates with silicic eruptions from the Katla volcanic system (SILK = silicic eruptions from Katla; Newton 1999a; Larsen 2000; et al., 2001). Newton (1999a, 1999b, 2000), further clarifies that while pumice from the Katla volcanic system is the most pervasive, several sources have likely also contributed to North Atlantic pumice including Öræfajökull (Iceland) and Jan Mayen (Boulton and Rhodes 1974). Despite early observations of local pumice rafting (e.g. 1947), there is no evidence of distally deposited Hekla pumice.

Katla is a glaciated central volcano in southern Iceland with the 600 km^2 ice cap, Mýrdalsjökull, covering its summit reaching up to 1490 m a.s.l. (Fig. A1; e.g., Schomacker et al., 2010). Based on geophysical echo-sounding data from Mýrdalsjökull, an ice thickness between 400 and 700 m is calculated for the caldera of Katla with a threshold at *c.* 700 m a.s.l. (Björnsson and Pálsson 2020). The volcano is located over 15 km inland from Iceland's current southern coastline. Katla has erupted approximately 300 times in the last 8400 years predominantly producing basaltic tephra (Óladóttir et al., 2008; Larsen et al., 2010). Of these eruptions, 21 are historical (during the last ~1100 years) and are often associated with jökulhlaups (e.g., Larsen 2000; Óladóttir et al., 2008; Larsen et al., 2010). Eighteen SILK layers, silicic tephra layers from Katla, have been identified from the ~300 Holocene eruptions (Larsen et al., 2001; Wastegård 2002; Thorsteinsdóttir et al., 2016; Wastegård et al., 2018 Table A1). The chemical characteristics of 18 SILK layers, (deposited between ~1600 and 9700 years BP), are used to facilitate better correlation of ocean-rafted pumice from Katla. (Newton 1999a; Larsen et al., 2001; Óladóttir et al., 2008; Thorsteinsdóttir et al., 2016; Wastegård et al., 2018). Pre-Holocene Katla eruptions (e.g. corresponding to the Skógar/Vedde Ash), distinct in chemistry and magnitude, in theory also produced pumice, however are not the focus of this study (Larsen et al., 2001).

The aim of this paper is to: i) analyze an archive of ocean-rafted pumice from Svalbard, collected during early occurrence mapping in 1958, with modern geochemical techniques ii) compare this geochemical data-set along with pumice from two other locations on Svalbard to relative sea level histories from each site to develop morphostratigraphic pumice horizons and iii) discuss the implications of ocean-rafted pumice horizons through the North Atlantic related to formation, transportation and deposition.

2. Setting

2.1. Lady Franklinfjorden, NE Svalbard

Located on the NW margin of Nordaustlandet, Lady Franklinfjorden is a *c.* 25 km long fjord hosting the largest outlet glacier of the Vestfonna ice cap (Fig. 1B). The regional bedrock is comprised of Precambrian siltstone, sandstone, and marble (Dallman 2015). The landscape is characterized by exposed weathered bedrock draped by flights of raised beaches and marine sediments. A relative sea level curve has been developed for the Storsteinhalvøya peninsula, located between Lady Franklinfjorden and the Hinlopen Strait (Fig. 2). Radiocarbon ages from 16 samples of driftwood, bivalve shells and whalebones (ranging from 2 to 44 m a.s.l.) have been used to constrain the last 10.5 ka of sea-level history for the region (Blake 1961a; Forman et al., 2004).

The curve constrains the lower 50 m of relative sea level although the regional marine limit is suggested to be higher (Blake 1961a; Forman et al., 2004). It is important to note that the relative sea level curve is constructed from samples taken over a wide region, wherein a prominent shoreline ranges from 6.6 to 9.4 m a.s.l. yet is associated with a synchronous palaeo-sea level (Blake 1961a). Three distinct horizons of ocean-rafted pumice have been described from this region (Blake 1961a).

Table 1
Pumice sample collection and occurrence corresponding to study site.

Location	Lady Franklinfjorden	Palanderbukta	Bjonahamna
Year	1958	2015	2019
Total samples	47	1	12
Collectors	WB & E. Tollén	WRF, ÓI & AS	WRF
Slag	Yes (below 2.5 m)	unknown	Yes (below 3 m)
Marine limit[a]	50 m a.s.l.	65 m a.s.l.	70 m a.s.l.
Km to RSL curve	25 km region	0	5
Sample range	2–10,5 m a.s.l.	20 m a.s.l.	2–17 m a.s.l.

[a] Marine limits according to Forman et al. (2004), Schomacker et al. (2019) and Sessford et al. (2015) respectively.

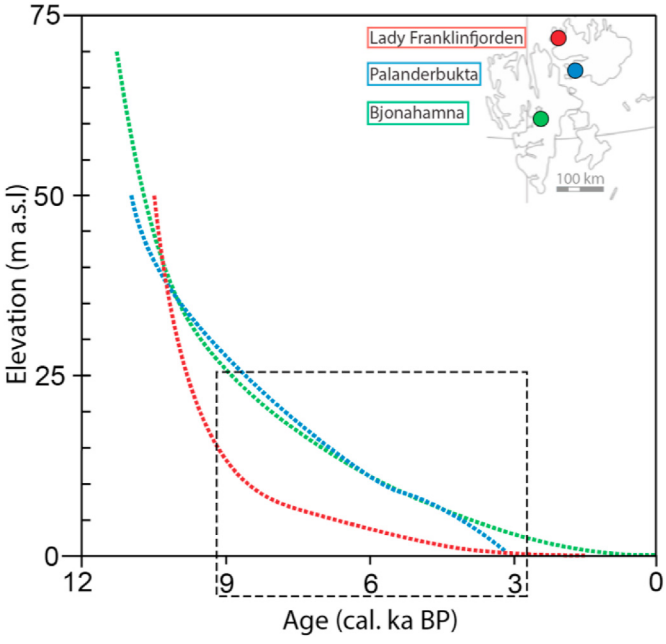

Fig. 2. Relative sea level curves for Lady Franklinfjorden, Palanderbukta and Bjonahamna according to Blake (1961a), Schomacker et al. (2019) and Sessford et al. (2015), respectively. Dashed inset box indicates the interval focused on in Fig. 4.

2.2. Palanderbukta, NE Svalbard

Located in south-central Nordaustlandet, Palanderbukta is a *c.* 20 km long tributary fjord to Wahlenbergfjorden (Fig. 2; Fig. A1). The coastal region is gently sloping and exhibits a flight of raised beach ridges intersected by a meltwater river draining to the north with run-off from local ice caps, Glitnefonna and Vegafonna. The regional bedrock geology is characterized by Carboniferous-Permian clastic sedimentary rocks including evaporates and carbonates as well as dolerites (Dallman 2015). Postglacial raised marine beach sediments extend up to c. 65 m a.s.l. and are exposed in a river section. Beach ridges exhibit low amplitude (0.5–1.0 m), and are predominantly composed of gravelly sediments (Schomacker et al., 2019). A relative sea level curve has been constructed from these raised beaches based on 10 radiocarbon ages from driftwood, bivalve shells and whalebones collected between 2 and 50 m a.s.l. (Fig. 2; Schomacker et al., 2019).

2.3. Bjonahamna, central Svalbard

Located in inner Isfjorden, Bjonahamna is a bay at the intersection between Sassenfjorden and Tempelfjorden, protected by a *c.* 1 km wide triangular peninsula, Bjonasletta (Fig. 1). The peninsula gently grades towards the NE, dominated by low amplitude (0.5 m high) beach ridges extending up to 45 m a.s.l. Ocean-rafted pumice has previously been described from Bjonasletta up to 21 m a.s.l. (Knape 1971;Salvigsen, 1984). The bedrock geology is characterized by Carboniferous-Permian carbonate rocks, evaporates and clastic sedimentary rocks (Dallman 2015). While no relative sea level curve has been established specifically for Bjonasletta, a Holocene uplift curve has been developed from a series of raised beaches at Fredheim, 5 km to the SE (Sessford et al., 2015). The region is suggested to have undergone at least 70 m of uplift relative to sea level over the last *c.* 11 ka. (Fig. 2; Sessford et al., 2015).

3. Methods

3.1. Field sampling

The pumice elevation from the Palanderbukta sample is obtained directly from Schomacker et al. (2019). A hand-held GPS (Garmin Montana 610) was used to determine the latitude and longitude of pumice samples from Bjonahamna. To acquire homogeneous accuracy, the elevation of each of the Bjonahamna samples was extracted from a 5-m-resolution digital elevation model produced by stereophotogrammetry on aerial photographs from 2009 (Norwegian Polar Institute, 2014). Average slopes in the surveyed regions do not exceed 10%, minimizing slope-induced error. Mean sea level is used as a vertical reference (Bondevik et al., 1995; Forman et al., 2004; Schomacker et al., 2019). We assume microtidal conditions (1–2 m range) since deglaciation for all sample locations (Egbert et al., 2004; Griffiths and Peltier 2008).

Field samples collected during the 1958 field campaign in Lady Franklinfjorden pre-date the use of hand-held GPS units. Pumice sample elevation was hand-leveled according to mean sea level with a WILD N-10 leveling instrument (Blake 1961a). A vertical error of 0.1 m is assumed for each sample from Lady Franklinfjorden with the exception of samples collected by the camp cook, E. Tollén. Larger errors bars correspond to these samples (with un-leveled sample elevation) however, pumice was collected between features with known elevation (e.g., between tidal gauge and bedrock knob, 7–9 m a.s.l.; Fig. A1).

3.2. Laboratory preparation and analysis

Ocean-rafted pumice samples (n = 60) were subsampled and fixed in epoxy, both in the form of slides and mounts for analysis. Points for microprobe analyses were plotted for a total of 10–20 locations from 1 to 3 randomly selected lines on the polished mounted subsamples (avoiding potentially affected rim areas; Guðmundsdóttir et al., 2011, 2012). Point analysis of 10 major elements was performed on all pumice samples at the University of Iceland on a JEOL JXA-8230 electron microprobe using an acceleration voltage of 15 kV, beam current of 10 nA and beam diameter of 10 μm. Lipari (rhyolitic obsidian) international standard was run periodically between samples, to monitor for instrumental drift and maintain consistency between measurements (Hunt et al., 1998). Data with geochemical anomalies resulting from partial analysis of microlites or glass impurities were omitted. Additionally, any analyses with elemental sums <95% were removed from the final dataset but retained in Table A1.

4. Results

We present descriptions, occurrence, elevation and major elemental geochemistry of ocean-rafted pumice for three regions in Svalbard, Lady Franklinfjorden, Palanderbukta and Bjonahamna. Our data are presented alongside previously published relative sea level curves respective to each region according to Blake (1961a), Schomacker et al. (2019) and Sessford et al. (2015; Table 1). Radiocarbon ages constraining relative sea level curves have all been (re-) calibrated and corrected for synchronizing the RSL curves according the SVALHOLA database (Table A1; Farnsworth et al., 2020).

4.1. Sample descriptions, occurrence and elevation

A total of 60 individual specimens of ocean-rafted pumice were collected on Svalbard's raised marine beaches during three distinct field campaigns; Lady Franklinfjorden 1958, Palanderbukta 2015 and Bjonahamna 2019 (Table 1; Fig. 3). Pumice samples range in color from dark-brown to greyish-black to grey (Fig. 3b-d; Salvigsen 1984).

Sample clast sizes range from lapilli (gravel ~20 mm) to bombs (cobbles ~150 mm; Schmid 1981). Clast morphology is dominated by equant, sub-rounded to rounded particles. Particle surfaces exhibit a range of micro-pitting and scalloped texture to smooth abraded surfaces.

There are variations in the occurrence elevation of ocean-rafted pumice within the three study regions. Pumice samples have been collected from beach ridges located as high as 20 m a.s.l. and as low as 2.75 m a.s.l. (Fig. 4). Porous anthropogenic ocean-rafted slag deposits were also found along active coasts between 2 and 3 m a.s.l during both the Lady Franklinfjorden field campaign in 1958 and the Bjonahamna campaign in 2019. These observations indicate a potential depositional range by wave action during a storm event. The 47 samples of pumice collected from Lady Franklinfjorden (LF-58) ranged from 2 to 10.5 m a.s.l. with high concentrations of pumice located on three horizons, roughly between 2 and 4, 6–7, and 8–10 m a.s.l (Fig. 4). Pumice collected from Bjonahamna (BH-19) ranged in elevation from 4 to 17 m a.s.l (Fig. 4). While several pumice and slag samples were collected between 2 and 4 m a.s.l., most were sampled from between 10 and 17 m a.s.l. (Fig. 4).

Despite early observations suggesting Bjonahamna pumice located as high as 21 m a.s.l. (Knape 1971), no pumice above 17 m a.s.l. was identified. The sole sample of pumice from Palanderbukta

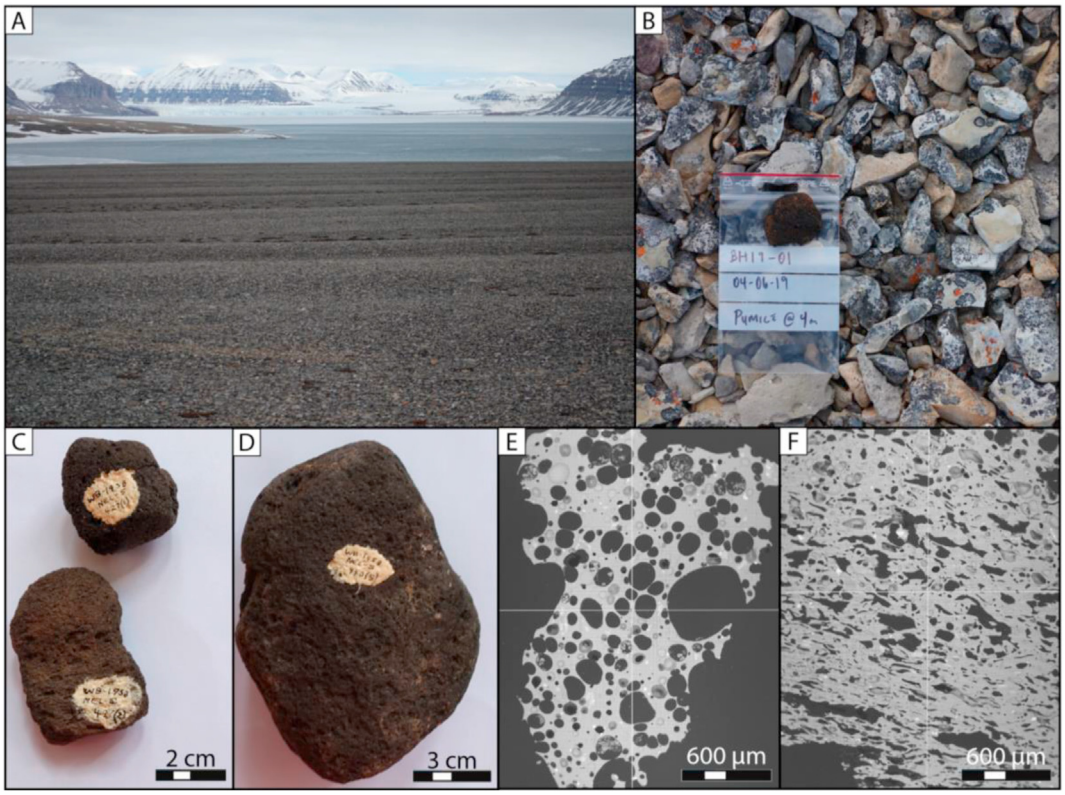

Fig. 3. Photomosaic of A) raised beach pumice sample site, Bjonahamna; B) field sample of pumice collected by W. Farnsworth at Bjonahamna, central Svalbard, 2019; C-D) archived ocean rafted pumice samples collected by W. Blake and E. Tollén at Lady Franklinfjorden, NE Svalbard, 1958; E-F) example imagery of pumice internal structure from the electron microprobe.

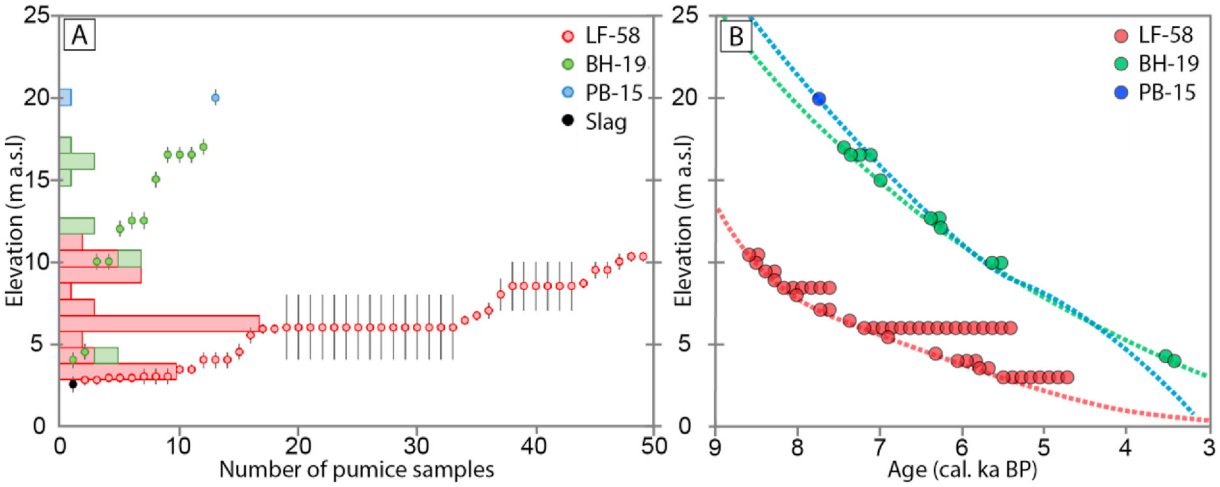

Fig. 4. A) Pumice samples according to elevation and sample site Lady Franklinfjorden (LF), Bjonahamna (BH) and Palanderbukta (PB). Black circle indicates occurrence elevation of modern rafted slag at Lady Franklinfjorden and Bjonahamna. Histogram of pumice occurrence by site with 1 m bin size. B) Sample elevation versus calibrated kilo-years before present (cal. ka BP) according to the relative sea level curves from each site (Blake 1961a; Sessford 2015; Schomacker et al., 2019, Fig. 2).

(PB-15) was collected at 20 m a.s.l. (Fig. 4; Schomacker et al., 2019). Variation in pumice sample quantity relates to the size of the region surveyed and the duration of the field campaign.

The rate and magnitude of postglacial isostatic uplift is heterogeneous in space and time across Svalbard (Forman et al., 2004). Variability is a result of the ice-cover duration and thickness of the Svalbard Barents Sea Ice Sheet, as well as the timing of its deglaciation during the Late Glacial and Early Holocene (Farnsworth et al., 2020). While Palanderbukta and Bjonahamna display relatively similar postglacial uplift histories through the Middle Holocene, thinner and/or shorter duration ice cover may have led to a more rapid exhaustion of isostatic rebound at Lady Franklinfjorden (Figs. 2 and 4B; Blake 1961a; Sessford et al., 2015; Schomacker et al., 2019).

4.2. Pumice geochemistry

All pumice samples were analyzed with the electron microprobe (10–20 points per clast) to gain major element composition for each ocean rafted particle. All samples are of intermediate-felsic composition, characterized as dacitic-trachydacitic with SiO_2 (percentage weight; % wt) values averaging 66% and ranging between 63 and 69% (Fig. 5A) akin to the chemical composition of the SILK layers from Katla. No significant variation is seen between the distinct sample locations. Geochemical composition of the ocean-rafted pumice samples is relatively consistent and overlaps with a previously established geochemical envelope of SILK eruptions from the Katla volcanic system (Newton 1999a; Larsen et al. 2001, 2010; Wastegård 2002; Thorsteinsdóttir et al., 2016; Wastegård et al., 2018). Investigations of Holocene SILK tephra layers from soil sections proximal to the Katla volcanic system suggest a total of 17 eruptions between 8.1 and 1.6 ka BP (Dugmore et al., 2000; Larsen et al., 2001, 2005; Óladóttir et al., 2005, 2008; Thorsteinsdóttir et al., 2016, Table 2). Furthermore, the Skopun tephra, an Early Holocene SILK layer identified in the Faroe Islands suggest the potential of older silicic eruptions not preserved in Iceland's soil records. While five of the SILK layers are constrained by radiocarbon dates, soil accumulation rates (SAR) provide an

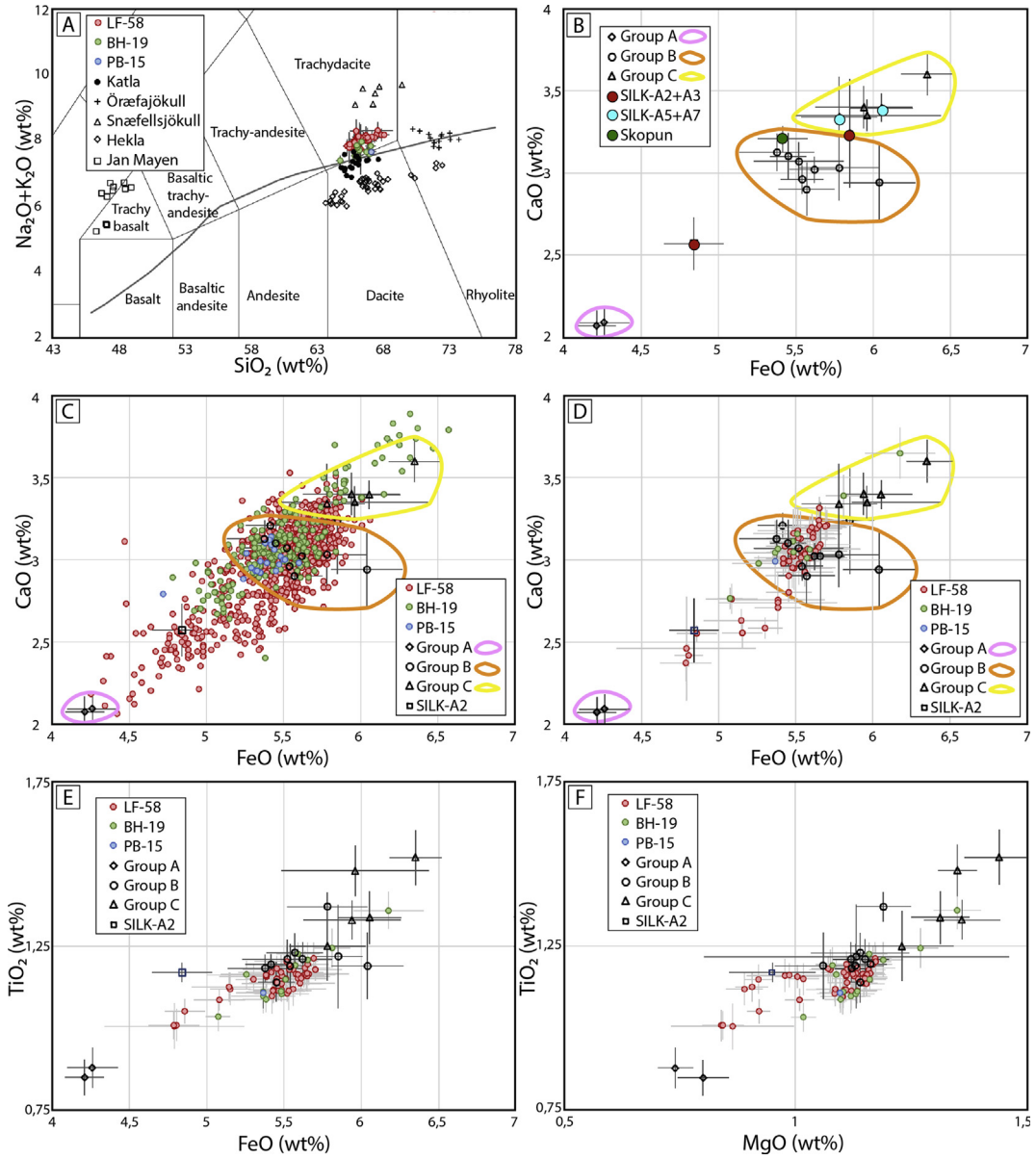

Fig. 5. A) Total Alkali-Silica plot of sample averages with 1σ error bars. Plots display the distribution of silica by weight percentage of ocean-rafted pumice sampled at Lady Franklinfjorden (LF-58), Bjonahamna (BH-19) and Palanderbukta (PB-15). Sample point cloud overlays dacitic to trachydacitic composition according to nomenclature by Le Bas et al. (1986) and straddles the Kuno-line (Kuno 1966). Geochemical composition is characteristic of SILK eruptions from the Katla volcanic system (Larsen et al., 2001; Thorsteinsdóttir et al., 2016; Meara et al., 2020). Comparative geochemistry presented for Jan Mayen (Gjerløw et al., 2016), Öræfajökull (Meara et al., 2020), Snæfellsjökull (Larsen et al., 2002), and Hekla (Meara et al., 2020). B) Weight percentage values of CaO plotted against FeO for 18 SILK layers according to groupings from Thorsteinsdóttir et al., (2016). SILK-A5 and SILK-A7 plot within Group C (Newton 1999a). Skopun plots within Group B (Wastegård et al., 2018). SILK-A3 plots indistinctly in either Group B or C, while SILK-A2 plots between Groups A and B (Óladóttir unpublished data; Table A1). Plotted SILK averages do not include SiO2 wt% values greater than 70% as this composition is not found within the pumice collection, however all values are included in Table A1. C-D) Svalbard point data and sample averages of CaO vs. FeO compared to SILK layer averages with 1σ error bars and layers grouped according to Thorsteinsdóttir et al. (2016). E-F) Pumice sample averages of TiO2 vs. FeO and TiO2 vs. MgO compared to SILK layer averages with 1σ error bars.

Table 2
Silicic Katla tephra layers with chemical groupings from Thorsteinsdóttir et al. (2016).

SILK Tephra	^{14}C age BP	Cal. yr BP & SAR age	Round Age	Age Reference	Groups
YN	1676 ± 12	1622 ± 40	1600	Dugmore et al. (2000)	B
UN	2660 ± 50	2850 ± 70	2800	Larsen et al. (2001)	C
MN	2975 ± 12	3230 ± 30	3200	Larsen et al. (2001)	B
LN	3139 ± 40	3440 ± 75	3400	Larsen et al. (2001)	B
N4		3920	3900	Óladóttir et al. (2008)	B
N3		4050	4100	Thorsteinsdóttir et al. (2016)	C
N2		4960	5000	Óladóttir et al. (2005)	C
N1[a]		5830	5800	Óladóttir et al. (2008)	B
A1[a]		6010	6000	Óladóttir et al. (2008)	B
A2[b]		6700	6700	Óladóttir et al. (2008)	X
A3[b]		6900	6900	Óladóttir et al. (2008)	B/C
A5[c]		7100	7100	Thorsteinsdóttir et al. (2016)	C
A7[c]		7180	7200	Óladóttir et al. (2008)	C
A8		7400	7400	Óladóttir et al. (2008)	B
A9		7500	7500	Óladóttir et al. (2008)	B
A11		8000	8000	Óladóttir et al. (2008)	A
A12		8100	8100	Óladóttir et al. (2008)	A
Skopun	8687 ± 156	9747 ± 190	9700	Wastegård et al. (2018)	B

[a] N1 & A1 have also been called T1 and T2 (Larsen et al., 2005).
[b] A2 & A3 grouping based on previously unpublished geochemistry (Supp. Table A1).
[c] A5 & A7 from Newton (1999a).

estimated time of eruption for the majority of the Holocene SILK layers (Table 2).

Based on grain and geochemical characteristics of 13 SILK layers, Thorsteinsdóttir et al. (2016) defined three distinct geochemical clusters (Group A, B and C) of glass composition by comparing the weight percentage of CaO to FeO (Fig. 5B; Thorsteinsdóttir et al., 2016). We add data from two SILK layers previously introduced by Newton (1999a; SILK-A5 and SILK-A7), one SILK layer described from the Faroe Islands (Skopun; Lind and Wastegård 2011; Wastegård et al., 2018) as well as two SILK layers previously unpublished (SILK-A2 and SILK-A3) to this group classification (Thorsteinsdóttir et al., 2016, Table 2).

The majority of the 18 eruptions (n = 9) have CaO weight percentages between 2,75 and 3,25 and FeO between 5,25 and 6,25 (Group B; Table 2; Fig. 5B). Five of the SILK layers have greater concentrations of CaO and FeO 3,25–4,75 and 5,5–6,5 respectively (Group C; Table 2; Fig. 5B). While there is no temporal relation within previous groupings, the two oldest eruptions (preserved in Iceland's soil archives) estimated to 8.1 and 8.0 ka BP exhibit low CaO and FeO weight percentage ranging from 2 to 2,5 and 4–4,5 respectively (Group A; Table 2; Fig. 5B).

While the geochemical data from SILK-A5 and SILK-A7 plot within Group C (Fig. 5B; Newton 1999a; Larsen et al., 2001), data from SILK-A2 and SILK-A3 do not clearly plot within any of the previously defined groups (Thorsteinsdóttir et al., 2016). The geochemical composition of SILK-A3 plots in between and overlaps the 1σ boundaries of Groups B and C (Fig. 5B). While the average of SILK-A2 plots between Group A and B, it plots outside the proposed groupings of Thorsteindóttir et al. (2016). We define SILK-A2 as a distinct geochemistry here termed Group X (Table 2). However, we are unable to determine whether SILK-A3 corresponds to Group B or Group C (Table 2). The Skopun SILK tephra plots within Group B (Wastegård et al., 2018). We compare the Svalbard point data as well as pumice sample averages to groupings A, B and C (Fig. 5C and D).

Major element geochemistry from ocean-rafted pumice samples collected on Svalbard's raised marine beaches plot within the geochemical averages of the SILK layers and within groupings defined by Thorsteinsdótter et al. (2016; Fig. 5C and D). Geochemistry from the majority of the Svalbard pumice samples have moderate CaO and FeO corresponding to Group B. Geochemistry from three pumice samples (n = 2 Bjonahamna; n = 1 Lady Franklinfjorden) exhibit enriched CaO and FeO plotting within Group C. No sample average from the Svalbard pumice plots directly within the Group A range, although pumice with these characteristics has been found in archaeological sites in Scotland (Newton 2001, 2004). Distinct geochemistry from four samples collected at Lady Franklinfjorden plot in-between Group A and Group B. The four pumice samples are geochemically distinct from Group B, however exhibit overlapping geochemistry associated with Group A. Plotted CaO and FeO wt % of the four samples overlaps with SILK-A2 (Fig. 5D).

5. Discussion

Geochemical distinction within the Svalbard dataset suggests the majority of analyzed ocean-rafted pumice falls within Groups B and C. While no samples appear to correspond to Group A, a series of four sample averages plot between group A and B (Fig. 6A). We suggest that there is a fourth geochemical group of the SILK layers, here termed cluster Group X (Table 2). The geochemical composition of the four Group X samples closely matches that of SILK-A2 (Fig. 6A; Table 3).

Statistics of major element composition is presented by grouping in Table 3. Plots exhibit co-variance in major elemental composition (Fig. 6A). Without stratigraphic context, ocean rafted pumice collected from Svalbard's raised beaches corresponds to a minimum of three geochemical distinct rafting events from the Katla volcanic system during the Middle to Late Holocene (Figs. 4–6; Table 3).

While comparing pumice sample averages (n = 10 to 20) to SILK layer data, the range in chemistry within a single grain is an important yet poorly understood factor (Fig. 6B). Pumice samples allow for numerous probe readings while tephra shards generally have space for a single point up to a few points. Ultimately a greater understanding of the variability of Holocene SILK geochemistry would be valuable in determining the rough ages of ocean-rafted pumice samples. However, these data do suggest the potential for distally deposited tephra to enhance our understanding of volcanic history and tephrochronology. While major elemental analysis was conducted on this ocean-rafted pumice dataset, the potential to further distinguishing eruption characteristics through trace element analysis or isotopic geochemistry remains to be investigated.

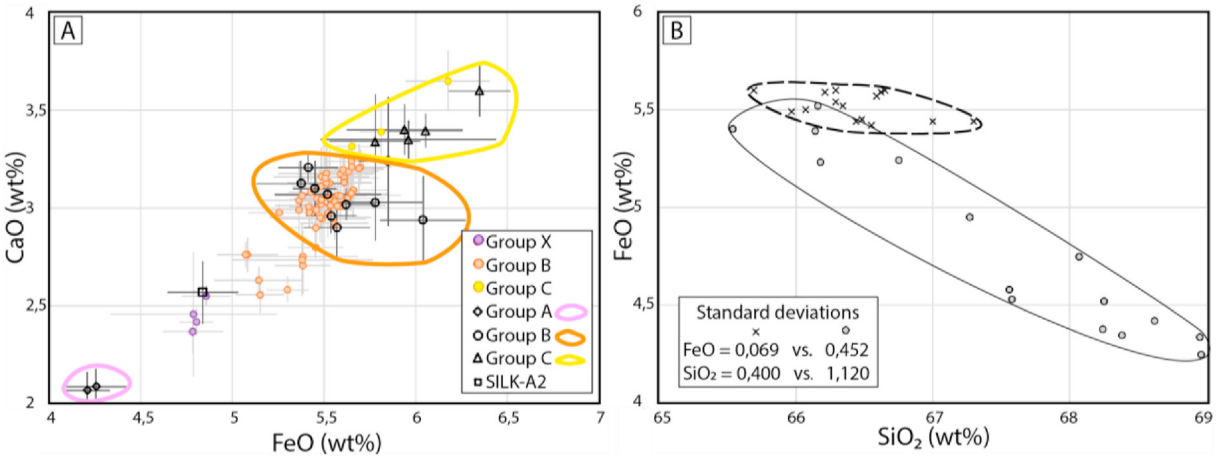

Fig. 6. A) Weight percentage values of CaO plotted against FeO of ocean rafted pumice averages from Svalbard compared to SILK layer averages grouped A, B and C by (Thorsteinsdóttir et al., 2016). All data presented with 1σ error bars. B) Plotted data with standard deviations from two Svalbard pumice samples highlighting the potential range in chemistry from a single clast/grain. While one sample displays a relatively precise cluster the other exhibits a larger geochemical range.

Table 3
Major element composition of Svalbard (Sval.) pumice compared to SILK layers according to groupings plotted in Fig. 6B. The groupings are based on the SILK layer geochemistry as suggested by Thorsteinsdóttir et al., (2016). The # column for Svalbard samples indicates sample number/analyzed points whereas for SILK it is number of layers.

			SiO_2	TiO_2	Al_2O_3	FeO	MnO	MgO	CaO	Na_2O	K_2O	P_2O_5	#
Group C	**Sval.**	**Avg.**	65,50	1,26	14,42	5,85	0,18	1,25	3,37	4,93	2,68	0,30	3/55
		S.D.	0,30	0,05	0,13	0,23	0,02	0,04	0,12	0,18	0,05	0,04	
	SILK	**Avg.**	64,27	1,38	14,01	6,02	0,20	1,34	3,42	4,37	2,61		SL = 5
		S.D.	0,57	0,08	0,19	0,28	0,03	0,08	0,14	0,17	0,10		
Group B	**Sval.**	**Avg.**	66,15	1,15	14,34	5,48	0,18	1,10	3,00	5,13	2,79	0,28	53/819
		S.D.	0,63	0,06	0,17	0,24	0,03	0,08	0,20	0,25	0,23	0,05	
	SILK	**Avg.**	65,10	1,21	13,97	5,56	0,18	1,13	3,03	4,47	2,74		SL = 9
		S.D.	0,56	0,06	0,18	0,20	0,03	0,06	0,13	0,16	0,10		
Group X	**Sval.**	**Avg.**	67,68	1,02	14,21	4,81	0,16	0,87	2,45	5,20	3,02	0,22	4/61
		S.D.	0,66	0,05	0,20	0,25	0,03	0,08	0,18	0,18	0,08	0,05	
	SILK	**Avg.**	67,51	1,17	14,56	4,84	0,16	0,95	2,57	4,64	2,99		SL = 1
		S.D.	0,57	0,03	0,15	0,19	0,13	0,09	0,16	0,17	0,05		
Group A	**Sval.**	**N.A.**											0/0
	SILK	**Avg.**	68,48	0,88	13,82	4,19	0,15	0,75	2,08	4,61	3,13	98,14	SL = 2
		S.D.	0,76	0,06	0,17	0,15	0,03	0,05	0,09	0,30	0,08	1,06	

5.1. Pumice as a constraint on relative sea-level history

Similar to most material used to constrain relative sea level, the deposition of ocean-rafted pumice may not necessarily occur at the actual sea level (Blake 1961a; Bondevik et al., 1995; Newton 1999a; Long et al., 2012). Pumice sample elevation likely corresponds to near or up to several meters above the actual sea level. Anthropogenic ocean-rafted slag material was also identified on raised beaches between 2 and 3 m a.s.l. during the Lady Franklinfjorden field campaign in 1958 (Blake 1961a) and at the Bjonahamna field campaign in 2019; Fig. A1). All sample regions are characterized by protected, inner-fjord environments with relatively short fetch and low-energy coastal conditions. However, observation of modern ocean-rafted material located 2–3 m above modern high-tide suggest the porous slag and pumice has the potential to be thrown above the actual sea level during stormy conditions. This process is not uncommon for driftage material (e.g., driftwood, whalebones, shell fragments and articulated juvenile *Astarte borealis*) used to date palaeo-shorelines (Dyke et al., 1991; Bondevik et al., 1995; Forman et al., 2004; Long et al., 2012). Bondevik et al. (1995) suggest modern deposition of driftwood and whalebones may occur 1.6–3.2 m above mean tide at the storm surf limit. Based on the occurrence elevation of rafted slag material and process understanding, conservatively we can assume pumice deposition along these protected coastlines may occur from up to 3 m above mean sea level to as low as 1 m below mean sea level. This elevation range is based on modern shoreline conditions and rates of sea level change. It is important to acknowledge that different processes could potentially re-deposit ocean-rafted material either above (e.g., sea-ice push) or below (e.g., coastal ice foot plucking, freeze-thaw processes and/or solifluction), its initial deposition (Blake 1961a; Dyke et al., 1991; Bondevik et al., 1995; Forman et al., 2004).

Based on the aforementioned assumptions, we plot ocean-rafted pumice from Svalbard on respective relative sea-level curves (Blake 1961a; Sessford et al., 2015; Schomacker et al., 2019) from each study site and compare the distribution to known silicic eruptions from the Katla volcanic system (Fig. 7A; Thorsteinsdóttir et al., 2016). Where pumice samples may correspond to more than one eruption based on sample elevation and projected age based on the relative sea-level curves, we assume pumice is more likely to have been thrown up above the sea level on a storm beach than deposited within the tidal range.

Holocene pumice rafting events are linked to phases of volcanic activity rather than specific volcanic events because in most cases, we are unable to distinguish between short interval eruptions

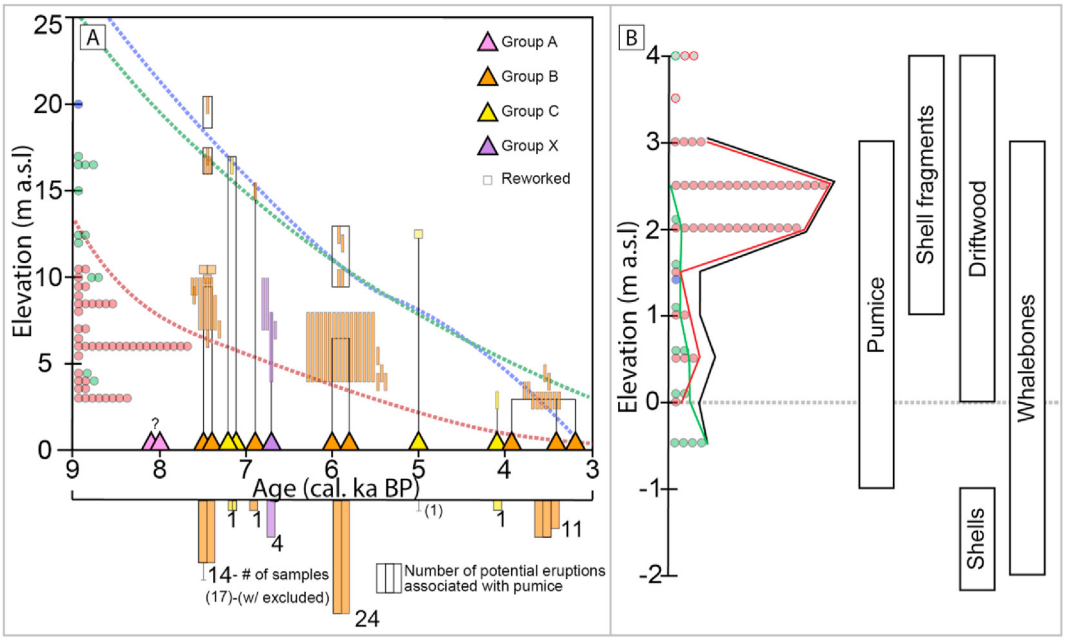

Fig. 7. A) Plot of ocean-rafted pumice from Svalbard compared to known silicic eruptions from the Katla volcanic system from the Middle and Late Holocene (Newton, 1999a; Thorsteinsdóttir et al., 2016; Óladóttir unpublished data). Triangles correspond to eruptions and are colored according to associated groupings based on CaO and FeO weight percentage (as in Figs. 5 and 6). Bars represent pumice samples and reflect elevation range; grouping according to color and are linked to respective relative sea level curves from Lady Franklinfjorden (Red; Blake 1961a), Palanderbukta (Blue; Schomacker et al., 2019) and Bjonahamna (Green; Sessford et al., 2015). Corresponding histogram of pumice samples associated with eight likely phases of eruptions. B) Plotted distribution of ocean-rafted pumice in relation to palaeo-shoreline. The deposition of ocean-rafted pumice is compared to other forms of driftage used to constrain relative sea level curves; e.g. driftwood, shell fragments, *in situ* shells and whalebones. (For interpretation of the references to color in this figure legend, the reader is referred to the Web version of this article.)

characterized by relatively similar geochemical composition (Table A1; Newton 1999a). For example, eruptions SILK-A1 and SILK-N1 at 6.0 and 5.8 ka BP, respectively, both exhibit moderate weight percentage values of CaO and FeO corresponding to Group B (Fig. 7A & Table A1). We describe this as the ~6 ka BP phase of eruption or pumice rafting event. The same applies to SILK-A11 and SILK-A12 (both with lower FeO and CaO compositions corresponding to Group A) at 8.1 and 8.0 ka BP referred to as the ~8 ka BP phase of eruption.

5.2. Pumice rafting events arriving to Svalbard

By combining geochemical composition and sample elevation in relation to respective relative sea-level histories, we identify eight distinct phases of eruption followed by pumice rafting events (Fig. 7A; Table A1). Svalbard pumice from Katla's eruption-triggered rafting events correlate to ~7.5 (SILK-A8/A9), ~7.2 (SILK-A5/A7), 6.9 (SILK-A3), 6.7 (SILK-A2), ~6 (SILK-N1/A1), 5 (SILK-N2), 4.1 (SILK-N3) and ~4-3 ka BP (SILK-N4/MN/LN).

While Blake (1961a) mapped three regional horizons consisting of high concentrations of ocean-rafted pumice, geochemical distinction within that dataset allows for the division of a 4th and 5th phase of eruption followed by an ocean-rafting (Fig. 7A). The majority of the Lady Franklinfjorden ocean-rafted pumice samples exhibit moderate CaO and FeO weight percentage (Group B) and correspond to eruptions and associated rafting events at ~7.5 ka BP (SILK-A8/A9), ~6 ka BP (SILK-N1/A1) and ~4-3 ka BP (SILK-N4/MN/LN). Four of the upper ocean-rafted pumice samples exhibit low CaO and FeO (Group X), however, not as reduced as Group A. The geochemical similarities of these four samples with SILK-A2 suggest they relate to a 4th eruption and rafting event at ~6.7 ka BP (SILK-A2). Furthermore, geochemical distinction of one the 10 pumice samples collected on the lower horizon (3–4 m a.s.l.) suggest origins of a 5th eruption at 4.1 ka BP corresponding to SILK-N3 (Group C; Figs. 5B and 7A).

Like the Lady Franklinfjorden dataset, other Svalbard pumice predominately exhibits moderate CaO and FeO, correlating with eruptions at c. 7.5 ka (SILK-A8/A9), ~6 ka (SILK-N1/A1) and 4-3 ka BP (SILK-N4/MN/LN). However, two samples from Bjonahamna with high CaO and FeO (Group C) likely correspond to a 6th and 7th eruption-rafting event from Katla at ~7.1 ka BP and 5 ka BP (SILK-A5/A7 and SILK-N2 respectively). The Group C pumice sampled at 16.5 m a.s.l. from Bjonahamna likely corresponds to a 6th distinct eruption-rafting event *c.* 7.1 ka BP. The second Group C sample collected at 13 m a.s.l. and 4 m above the palaeo-sea level is presumably reworked, falling outside of the *in situ* range we define (Fig. 7). However, the geochemical composition appears distinct even inside of the Group C range. Both this Bjonahamna pumice sample and SILK-N2 exhibit the greatest weight percentage of CaO and FeO making them relatively distinct from the rest of Group C (Fig. 6A). Although the sampled elevation may not reflect *in-situ* deposition, it seems to correlate with a 7th rafting event arriving to Svalbard. Finally, and due to rapid isostatic uplift through the Middle Holocene at Bjonahamna, it is possible to discern a potential 8th rafting event based on the morphostratigraphic relationship between the upper five samples. The upper Group C sample, collected from an elevation between Group B samples at 16.5 m a.s.l. and 15 m a.s.l. suggests that the lower Group B sample likely relates to a rafting event after the upper Group C sample. This corresponds to SILK-A3 at 6.9 ka BP. Although it is possible Group B samples from Lady Franklinfjorden also were deposited during this 6.9 ka BP rafting event, the lower uplift rates and sample elevation uncertainty do not allow for the same morphostratigraphic precision.

A total of four samples (1 from BH-19 and 3 from LF58) from our 60-sample dataset fall outside of the likely pumice deposition

elevation range (indicated boxes or grey circles; Fig. 7). There is a possibility that the three excluded samples from Lady Franklinfjorden found at 10 m and 10.5 m a.s.l. (3.5 m and 4 m above palaeo-sea-level) correspond to pumice rafting events which occurred prior to the 8-ka BP phase of eruption. However, little is known about Katla's SILK eruptions history during the Early Holocene, with the exception of the Skopun tephra identified in the Faroe Islands (Larsen et al., 2001; Óladóttir et al., 2007; Lind and Wastegård 2011; Thorsteinsdóttir et al., 2015; Wastegård et al., 2018). Ultimately, it is unclear if the pumice at these sites can be deposited 4 m a.s.l., if they have been reworked or if they relate to some other less known phase of eruption.

5.3. Limitations and potentials of ocean-rafted pumice

Pumice samples fit well with respective relative sea-level curves given the spatial range of the Lady Franklinfjorden curve and the 5-km offset of the sea-level curve from Bjonahamna. However, similar to other forms of driftage used to constrain palaeo-sea level, ocean-rafted pumice has its limitations. A vertical resolution of 3–4 m related to depositional processes is similar to driftwood, whalebones and shells. However, the inherent small and light pumice clasts maybe more susceptible to post-depositional reworking compared to logs of driftwood and large whalebones. Similar to driftwood, other factors like sea-ice persistence, transgressions and preservation potential may influence the occurrence and distribution of ocean-rafted pumice (Häggblom 1982; Funder et al., 2011; Romundset and Lakeman 2019). Based on our estimate of a 4-m depositional range (3+ m and 1- m below mean tide) for our three study sites, a total five of the 60 samples (~8%) were possibly subject to post-depositional processes.

While this study presents a detailed survey of pumice occurrence on raised marine beaches at several locations from Svalbard, higher resolution records with more extensive postglacial uplift should be targeted in future studies (e.g., Kong Karls Land or mainland Scandinavia). Additionally, a transect of study sites through the North Atlantic (from Iceland to Svalbard) may signal if there are more volcanic provinces responsible for Holocene rafted pumice, which never managed to arrive to Svalbard's shores (e.g., Beerenberg at Jan Mayen, or other volcanic systems like Hekla in Iceland), although there is currently no evidence from wider studies that have included pumice from the British Isles, mainland Norway and NW Iceland (e.g. Newton 1999a). Furthermore, due to occurrence of anthropogenic ocean-rafted slag proximal to modern coastlines, little focus was given to the active shoreline. However, it would be valuable to target this environment in future investigations to try to identify ocean-rafted pumice deposits from historical volcanic eruptions. This type of investigation would provide perspective on the scale and actual quantities of ocean-rafted pumice traveling around in the North Atlantic as result of such an eruption. Deposits from SILK-A11, A12 and the Skopun eruptions are not clearly represented in this dataset from Svalbard. However, potential phases of Early Holocene pumice rafting are suggested by previous observations of higher elevation Bjonahamna pumice (21 m a.s.l., 5 m above and potentially 1 ka older than the uppermost analyzed sample) as well as the upper three samples from Lady Franklinfjorden. More work is needed targeting these earlier (and modern) shorelines to develop a more holistic understanding of the distal deposition of ocean rafted pumice through the Holocene. Furthermore, investigations comparing porosity, vesicle structure and density from pumice identified on Svalbard to local pumice on Iceland may convey the uniqueness of these distally deposited particles.

Although the full Holocene history of Katla's silicic volcanism is not expressed in the raised beaches of Svalbard, these pumice investigations double the occurrence of distally deposited Holocene tephra horizons identified in Svalbard (Kekonen et al., 2005; Wastegård and Davies 2009; D'Andrea et al., 2012; van der Bilt et al., 2017). While the widespread Vedde Ash has been identified in marine records in the North Atlantic and Fram Strait (Zamelczyk et al., 2012; Gjerløw et al., 2016), no previous deposits of the Katla volcanic system have been identified on Svalbard.

Deposits from pre-historic Holocene eruptions, although widespread and relatively constrained, are not necessarily well-dated (Óladóttir et al., 2008). There is the potential to improve the timing of known volcanic eruptions with more investigations of ocean-rafted pumice within the North Atlantic, and specifically linking pumice occurrence with well-constrained relative sea-level curves (Romundset et al., 2018). Apart from important marker tephra layers, that are radiocarbon dated on associated organic material, most pre-historic Holocene eruptions are roughly dated by soil accumulation rates, which assumes constant accumulation between tephra marker layers (Óladóttir et al., 2008). Five of the SILK layers are constrained by an associated radiocarbon age (Dugmore et al., 2000; Larsen et al., 2001; Wastegård et al., 2018, Table 2). Combining ocean rafted pumice with well-constrained relative sea-level curves maybe a potential form of dating such eruptions. This is particularly true for Early Holocene eruptions poorly preserved in Iceland's soil sections (Newton 1999a; Larsen and Eiríksson 2007).

5.4. Pumice, jökulhlaups and Holocene ice cap cover

Nearly 100 silicic tephra layers have been identified from Holocene soil sections in Iceland (Larsen and Eiríksson 2007). These deposits are predominantly a result of eruptions from seven central volcanos: Hekla, Torfajökull, Öræfajökull, Askja, Snæfellsjökull, Eyjafjallajökull and Katla (Óladóttir et al., 2020). One of the likely factors governing the prevalence of Katla's silicic pumice throughout the North Atlantic during the Holocene relates to the frequency and magnitude of eruption-driven jökulhlaups from the Mýrdalsjökull ice cap (Gröndal et al., 2005; Larsen et al., 2005; Smith and Dugmore 2006; Schomacker et al., 2010). These flood events facilitate the episodic transport of pumice from the inland caldera, to beyond the coast of Iceland. Subsequently it enters the regional ocean surface currents either counter clockwise towards the west and north off Iceland or to the east along the southern coast and into the NC and WSC (Fig. 1; Tómasson 1996; Newton 1999a; Valdimarsson and Malmberg 1999; Smith and Dugmore 2006).

While there are other plausible ways to get a pumice clast from Katla to Svalbard (e.g., air-fall deposition, reworked from a river-bank or transported by a landslide), the extensive quantities and coarse nature of ocean-rafted pumice throughout the North Atlantic suggests these are less probable scenarios. We regard eruption-driven jökulhlaups, creating large pumice rafting events through the North Atlantic, the most reasonable contributor of pumice horizons (clasts over 15 cm with concentrations up to 10 particles per square meter) on Svalbard's raised beaches. Furthermore, speculations of whether pumice formed during an eruption into a lake filling the (unglaciated) Katla caldera would not result in distinct pumice horizons on Svalbard's raised beaches.

If we assume a pumice rafting event (consisting of Katla's silicic pumice) in the North Atlantic requires a jökulhlaup to flush the large quantities of clasts to the sea, a glacio-volcanic (phreato-magmatic) interaction accompanied by substantial melting is required within the Katla caldera (Tómasson 1996). Our dataset of distally deposited ocean-rafted pumice from Katla found on

Svalbard, together with previous studies elsewhere in the North Atlantic (e.g. Newton 1999a; Romundset and Lakeman 2019), indicates pumice rafting events throughout the Middle and Late Holocene, thus implies a glaciated Katla caldera and the persistence of a substantial portion the Mýrdalsjökull ice cap through the Holocene.

Glaciers in Iceland exhibited their minimum extent sometime during the Holocene thermal maximum (HTM) between 7.9 and 5.5 ka BP (Striberger et al., 2012; Geirsdóttir et al., 2013). Synchronous with elevated northern hemisphere summer insolation, terrestrial and lacustrine proxy records suggest summer temperatures during this period were on the order of 2.5–3.2 °C greater than present (Caseldine et al., 2006; Harning et al., 2020). Models project Holocene glaciers in Iceland were non-existent or greatly reduced through the Middle Holocene (Flowers et al., 2008; Anderson et al., 2019).

Our pumice results add to the mounting evidence from independent field studies suggesting the persistence of some of Iceland's ice caps through the Holocene, underlining the intricacies of Iceland's Holocene glacial history (Dugmore 1989; Dugmore and Sugden 1991; Stötter et al., 1999; Kirkbride & Dugmore 2001, 2006; Larsen et al., 2005; Gröndal et al., 2005; Óladóttir et al., 2007; Brynjólfsson et al., 2015; Thorsteinsdóttir et al., 2016). While current models do not fully grasp the complexities of Holocene glaciers on Iceland, these data may reflect the critical driving role of winter precipitation in sustaining their mass balance. We recommend investigations modeling Holocene ice cover in Iceland to incorporate these data into projections for holistic and data-driven simulations which will ultimately improve projection of future ice-cap demise (Anderson et al., 2019). Modeling the extent of the Mýrdalsjökull ice cap required to produce jökulhlaups of various scales during the Middle Holocene would be a valuable contribution to constraining the minimum extent of Holocene ice caps in Iceland.

While an eruption-driven jökulhlaup from Katla has, and will certainly impact settlements in the region and watershed (Tómasson 1996; Smith and Dugmore 2006), the subsequent pumice rafting event has the potential to disturb ocean traffic within the greater North Atlantic. Constrained by historic observations of the 1918 jökulhlaup from Mýrdalsjökull (Tomásson, 1996), models could be used to investigate the scale of pre-historic jökulhlaups and the quantities of flushed sediment to the North Atlantic. Pumice frequency identified on raised beaches could be used to reconstruct the extent and volume of ocean-rafted pumice related to specific eruptions (Blake 1961a; Salvigsen 1984; Newton 1999a). This in turn may provide constraint on the scale of jökulhlaup and conditions during pre-historic volcanic eruptions.

6. Summary and conclusions

Although not a silver-bullet to constraining palaeo-sea-level, we conclude that ocean-rafted pumice is a beneficial and underutilized tool, which should be added to the list of valuable constraints for palaeo-sea level reconstruction (alongside driftwood, bivalve shells, whalebones and isolation basins). Geochemistry from the 60 analyzed samples of ocean rafted pumice presented in this study corroborates evidence that the Katla volcanic system is the key contributor to distally deposited ocean-rafted pumice through the Middle and Late Holocene within the North Atlantic (Newton 1999a). We suggest eight likely phases of distinct ocean-rafted, silicic pumice arriving to Svalbard's shores during the Middle and Late Holocene based on geochemically linked and stratigraphically supported evidence. Investigations of ocean-rafted pumice show potential to not only constrain the timing of palaeo-sea levels, but help to actually constrain the age of previously un-dated Holocene eruptions. Our data supports evidence that the Mýrdalsjökull ice cap likely survived the Holocene thermal maximum on Iceland, given eruption-triggered-jökulhlaups critically facilitated the arrival of Katla pumice to beyond the coast of Iceland (Newton 1999a; Gröndal et al., 2005; Larsen et al., 2005; Óladóttir et al., 2007). This multidisciplinary investigation highlights the potential of ocean-rafted pumice and its ability to enhance our understanding of postglacial relative sea level as well as palaeo-volcanic/ice cap conditions.

Author contributions

W.R.F., Ó.I. and E.R.G conceived this work while W.R.F. and W.B. collected field samples. A.S. analyzed elevation data. W.R.F., E.R.G., G.L., A.N., B.A.Ó. and M.K. conducted electron microprobe analysis and interpretation. All authors contributed with interpretation and discussion of results. WRF wrote the paper with all co-authors contributing.

Declaration of competing interest

The authors declare that they have no known competing financial interests or personal relationships that could have appeared to influence the work reported in this paper.

Acknowledgments

E. Tollén and H.D. Gunnarsdóttir are thanked for field assistance and sample collection during the respective 1958 and 2019 field campaigns. M. Retelle, J. Smol and E. Blake are thanked for their support with accessing the 1958 Lady Franklinfjorden archive. The 1958 fieldwork was supported by the Foreign Field Research Program, National Academy of Science, USA, as well as the Geography Branch, Office of Naval Research, USA, and by Profs. G. Hoppe, V. Schytt, R. Goldthwait, and G. Liljequist (to WB). Recent field campaigns were funded by the Carlsberg Foundation (CF14-0756 to AS), The Svalbard Environmental Protection Fund (Project 16/35 to WRF), and the Department of Arctic Geology, University Centre in Svalbard (to ÓI). We acknowledge funding from the Nordic Volcanological Center at the University of Iceland for data analysis. S. Steinþórsson, R.H. Rúnarsdóttir and G.H. Guðfinnsson are kindly acknowledged for support with sample preparation and the electron microprobe. We kindly acknowledge two anonymous reviewers for thier constructive comments. Farnsworth would like to thank J. Moreno for providing an early introduction to this topic.

Appendix A. Supplementary data

Supplementary data to this article can be found online at https://doi.org/10.1016/j.quascirev.2020.106654.

References

Anderson, L.S., Geirsdóttir, Á., Flowers, G.E., Wickert, A.D., Aðalgeirsdóttir, G., Thorsteinnsson, T., 2019. Controls on the lifespan of Icelandic ice caps. Earth Planet Sci. Lett. 527, 11578.

Abbott, P.M., Jensen, B.J.L., Lowe, D.J., Suzuki, T., Veres, D., 2020. Crossing new frontiers: extending tephrochronology as a global geoscientific research tool. J. Quat. Sci. 35, 1–8.

Bäckström, H., 1890. Über angeschwemmte Bimssteine und Schlacken der nordeuropäischen Küsten. Bihang til Kungl. Svenska Vetenskaps-Akademiens Handlingar 16 (2–5), 1–43.

Balchin, W.G.V., 1941. The raised features of billefjord and sassenfjord West Spitsbergen. Geography Journal 97, 364–376.

Binns, R.E., 1967. Drift pumice on post-glacial raised shorelines of northern Europe. Acta Borealia A 24, 1–63.

Binns, R.E., 1971. The Distribution and Origin of Pumice on Post-glacial Shorelines in

Northern Europe and the Western Arctic (MSc. Thesis). Abersytwyth University.
Binns, R.E., 1972. Composition and derivation of pumice on post-glaciation strandlines in northern Europe and western Arctic. Geol. Soc. Am. Bull. 83 (8), 2303–2324.
Blake Jr., W., 1961a. Radiocarbon dating of raised beaches in Nordaustlandet, Spitsbergen. In: Raasch, G.O. (Ed.), Geology of the Arctic. University of Toronto Press, Toronto, pp. 133–145.
Blake Jr., W., 1961b. Russian settlement and Land rise in Nordaustlandet, spitsbergen. Arctic 14 (2), 101–111.
Blake Jr., W., 1970. Studies of glacial history in arctic Canada. I. Pumice, radiocarbon dates and differential post-glacial uplift in eastern Queen Elizabeth Island. Can. J. Earth Sci. 7 (2), 634–644.
Björnsson, H., Pálsson, F., 2020. Radio-echo soundings on Icelandic temperate glaciers: history of techniques and findings. Ann. Glaciol. 1–10.
Bondevik, S., Mangerud, J., Ronnert, L., Salvigsen, O., 1995. Postglacial sea-level history of Edgeøya and barentsøya, eastern svalbard. Polar Res. 14, 153–180.
Boulton, G.S., Rhodes, M., 1974. Isostatic uplift and glacial history in northern Spitsbergen. Geology Magazine 111 (6), 481–500.
Bryan, S.E., Cook, A.G., Evans, J.P., Hebden, K., Hurrey, L., Colls, P., Jell, J.S., Weatherley, D., Firn, J., 2012. Rapid, long-distance dispersal by pumice rafting. PloS One 7 (7), e40583.
Bryan, S.E., Cook, A., Evans, J.P., Colls, P.W., Wells, M.G., Lawrence, M.G., Jell, J.S., Greig, A., Leslie, R., 2004. Pumice rafting and faunal dispersion during 2001–2002 in the southwest Pacific: record of a dacitic submarine explosive eruption from Tonga. Earth Planet Sci. Lett. 227, 135–154.
Brynjólfsson, S., Schomacker, A., Ingólfsson, Ó., Keiding, J.K., 2015. Cosmogenic 36Cl exposure ages reveal a 9.3 ka BP glacier advance and the Late Weichselian-Early Holocene glacial history of the Drangajökull region, northwest Iceland. Quat. Sci. Rev. 126, 140–157.
Carey, R., Soule, S.A., Manga, M., White, J.D.L., McPhie, J., Wysoczanski, R., Jutzeler, M., Tani, K., Yoerger, D., Fornari, D., Caratori-Tontini, F., Houghton, B., Mitchell, S., Ikegami, F., Conway, C., Murch, A., Fauria, K., Jones, M., Cahalan, R., McKenzie, W., 2018. The largest deep-ocean silicic volcanic eruption of the past century. Science Advances 4, e1701121.
Caseldine, C., Langdon, P., Holmes, N., 2006. Early Holocene climate variability and the timing and extent of the Holocene thermal maximum (HTM) in northern Iceland. Quat. Sci. Rev. 25, 2314–2331.
Cashman, K.V., Fiske, R.S., 1991. Fallout of pyroclastic Debris from submarine volcanic eruptions. Science 253, 275–280. https://doi.org/10.1126/science.253.5017.275.
Dallmann, W.K., 2015. Geoscience Atlas of svalbard. Norsk Polarinstitutt Rapportserie 148, 1–292.
Davies, S.M., 2015. Cryptotephras: the revolution in correlation and precision dating. J. Quat. Sci. 30 (2), 114–130.
D'Andrea, W.J., Vaillencourt, D.A., Balascio, N.L., Werner, A., Roof, S.R., Retelle, M., Bradley, R.S., 2012. Mild Little Ice Age and unprecedented recent warmth in an 1800 year lake sediment record from Svalbard. Geology 40, 1007–1010.
De Geer, G., 1896. Rapport om den svenska geologiska expeditionen till Isfjorden på Spitsbergen sommaren 1896. Ymer. Årg 16, 259–266.
Donner, J.J., West, R.G., 1957. The quaternary geology of brageneset, Nordaustlandet, spitzbergen. Nor. Polarinst. Skr. 109, 1–29.
Dugmore, A.J., Thompson, P.I.J., Streeter, R.T., Cutler, N.A., Newton, A.J., Kirkbride, M.P., 2020. The interpretive value of transformed tephra sequences. J. Quat. Sci. 35, 23–28.
Dugmore, A.J., 1989. Tephrochronological studies of Holocene glacier fluctuations in south Iceland. in Oerlemans, J. (ed.), Glacier Fluctuations and Climatic Change, Kluwer Academic Publishers, Dordrecht, Netherlands, 37–55.
Dugmore, A.J., Newton, A.J., Larsen, G., Cook, G.T., 2000. Tephrochronology, environmental change and the Norse settlement of Iceland. Environ. Archaeol. 5, 21–34.
Dugmore, A.J., Sugden, D.E., 1991. Do the anomalous fluctuations of Solheimajökull reflect ice-divide migration? Boreas 20, 105–111.
Dyke, A.S., Morris, T.F., Green, D.E.C., 1991. Postglacial tectonic and sea-level history of the central Canadian Arctic. Geol. Surv. Can. Bull. 397, 1–56.
Egbert, G.D., Ray, R.D., Bills, B.G., 2004. Numerical modelling of the global semidiurnal tide in the present day and in the last glacial maximum. Journal of Geophysical Research 109, C03003.
Fang, X., Zeng, Z., Hu, S., Li, X., Chen, Z., Chen, S., Zhu, B., 2019. Origin of pumice in sediments from the middle okinawa trough: constraints from whole-rock geochemical compositions and Sr-Nd-Pb Isotopes. J. Mar. Sci. Eng. 7, 462.
Farnsworth, W.R., Allaart, L., Ingólfsson, Ó., Alexanderson, H., Forwick, M., Noormets, R., Retelle, M., Schomacker, A., 2020. Holocene glacial history of Svalbard - status, perspectives and challenges. Earth Sci. Rev. 208, 103249.
Feyling-Hanssen, R.W., 1955. Stratigraphy of the marine late pleistocene of billefjorden. Nor. Polarinst. Skr. 107, 187.
Fisher, R.V., Schmincke, H.-U., 1984. Pyroclastic Rocks. Springer Verlag, Berlin, p. 472.
Flowers, G.E., Björnsson, H., Geirsdóttir, Á., Miller, G.H., Black, J.L., Clarke, G.K.C., 2008. Holocene climate conditions and glacier variation in central Iceland from physical modelling and empirical evidence. Quat. Sci. Rev. 27, 797–813.
Forman, S.L., Lubinski, D.J., Ingólfsson, Ó., Zeeberg, J.J., Snyder, J.A., Siegert, M.J., Matishov, G.G., 2004. A review of postglacial emergence on svalbard, Franz Josef Land and Novaya Zemlya, northern Eurasia. Quat. Sci. Rev. 23, 1391–1434.
Funder, S., Goosse, H., Jepsen, H., Kaas, E., Kjær, K.H., Korsgaard, N.J., Larsen, N.K., Linderson, H., Lysså, A., Möller, P., Olsen, J., Willerslev, E., 2011. A 10,000-year record of arctic ocean sea-ice variability—view from the beach. Science 333, 747–750.
Guðmundsdóttir, E.R., Larsen, G., Eiríksson, J., 2012. Tephra stratigraphy on the North Icelandic shelf: extending tephrochronology into marine sediments off North Iceland. Boreas 41 (4), 718–734.
Guðmundsdóttir, E.R., Eiríksson, J., Larsen, G., 2011. Identification and definition of primary and reworked tephra in Late glacial and Holocene marine shelf sediments off North Iceland. J. Quat. Sci. 26, 589–602.
Gröndal, G.O., Larsen, G., Elefsen, S., 2005. Stærðir forsögulegra hamfaraflóða í Markarfljóti – mæling á farvegum neðan Einhyrningsflata. (Magnitudes of prehistoric catastrophic floods in the Markarfljót river – survey of flood channels south of Einhyrningsflatir.). In: Guðmundsson, M.T., Gylfason, Á.G. (Eds.), Hættumat Vegna Eldgosa Og Hlaupa Frá Vestanverðum Mýrdalsjökli Og Eyjafjallajökli. The National Commissioner of the Icelandic Police and the University Press, Reykjavík, pp. 99–104.
Gjerløw, E., Haflidason, H., Pedersen, R.B., 2016. Holocene explosive volcanism of the Jan Mayen (island) volcanic province, North-Atlantic. J. Volcanol. Geoth. Res. 321, 31–43.
Geirsdóttir, Á., Miller, G.H., Larsen, D.J., Ólafsdóttir, S., 2013. Abrupt Holocene climate transitions in the northern North Atlantic region recorded by synchronized lacustrine records in Iceland. Quat. Sci. Rev. 70, 48–62.
Griffiths, S.D., Peltier, W.R., 2008. Megatides in the arctic ocean under glacial conditions. Geophysical research letters 35, L08605.
Harning, D.J., Curtin, L., Geirsdóttir, Á., D'Andrea, W.J., Miller, G.H., Sepúlveda, J., 2020. Lipid biomarkers quantify Holocene summer temperature and ice cap sensitivity in Icelandic lakes. Geophys. Res. Lett. 47, 2019GL085728.
Hunt, J.B., Clift, P.D., Lacasse, C., Vallier, T.L., Werner, R., 1998. Inter-laboratory comparison of electron probe microanalysis of glass geochemistry: proceedings of the ODP. Scientific Results 152, 85–91.
Häggblom, A., 1982. Driftwood as an indicator of sea ice conditions. Geogr. Ann. 64 A, 81–94.
Jutzeler, M., Marsh, R., van Sebille, E., Mittal, T., Carey, R.J., Fauria, K.E., Manga, M., McPhie, J., 2020. Ongoing dispersal of the 7 August 2019 pumice raft from the Tonga arc in the southwestern Pacific Ocean. Geophys. Res. Lett. 47, e1701121.
Kalliokoski, M., Guðmundsdóttir, E.R., Wastegård, S., 2020. Hekla 1947, 1845, 1510 and 1158 tephra in Finland: challenges of tracing tephra from moderate eruptions. J. Quat. Sci. 35 (6), 803–816. https://doi.org/10.1002/jqs.3228.
Kekonen, T., Moore, J., Perämäki, P., Mulvaney, R., Isaksson, E., Pohjola, V., van de Wal, R.S.W., 2005. The 800-year long ion record from the Lomonosovfonna (Svalbard) ice core. Journal of Geophysical Research 110, D07304.
Kuno, H., 1966. Lateral variation of basalt magma across continental margins and island Arcs. Paper 66-15. geological survey of Canada, p. 317.
Kirkbride, M.P., Dugmore, A.J., 2001. Timing and significance of mid-Holocene glacier advances in northern and central Iceland. J. Quat. Sci. 16, 145–153.
Kirkbride, M.P., Dugmore, A.J., 2005. Late Holocene solifluction history reconstructed using tephrochronology. Geological Society, London, Special Publications 242 (1), 145–155.
Kirkbride, M.P., Dugmore, A.J., 2006. Responses of mountain ice caps in central Iceland to Holocene climate change. Quat. Sci. Rev. 25, 1692–1707.
Knape, P., 1971. C-14 Dateringar Av Höjda Strandlinjer, Synkrona Pimpstensnivåer Och Iakttagelser Av Högsta Kustlinjen På Svalbard.. unpublished Licentiate thesis Stockholm University Department of Physical Geography, p. 142.
Kokelaar, P., 1986. Magma-water interactions in subaqueous and emergent basaltic volcanism. Bull. Volcanol. 48, 275–289.
Larsen, G., 2000. Holocene eruptions within the Katla volcanic system, south Iceland, Characteristics and environmental impact. Jokull 49, 1–28.
Larsen, G., Newton, A.J., Dugmore, A.J., Vilmundardóttir, E.G., 2001. Geochemistry, dispersal, volumes and chronology of Holocene silicic tephras from the Katla volcanic system, Iceland. J. Quat. Sci. 16, 119–132.
Larsen, G., Smith, K., Newton, A.J., Knudsen, Ó., 2005. Jökulhlaup til vesturs frá Mýrdalsjökli: Ummerki um forsöguleg hlaup niður Markarfljót. (Volcanogenic floods towards west from Mýrdalsjökull ice cap: indications of prehistoric floods in the Markarfljót river.). In: Magnús, T., Guðmundsson og, Ágúst G. Gylfason (Eds.), Hættumat Vegna Eldgosa Og Hlaupa Frá Vestanverðum Mýrdalsjökli Og Eyjafjallajökli. The National Commissioner of the Icelandic Police and the University Press, Reykjavík, pp. 75–98.
Larsen, G., Eiríksson, J., 2007. Late Quaternary terrestrial tephrochronology of Iceland e frequency of explosive eruptions, type and volume of tephra deposits. J. Quat. Sci. 23, 109–120.
Larsen, G., 2010. Katla: tephrochronology and eruption history. Dev. Quat. Sci. 13, 23–49.
Le Bas, M.J., Le Maitre, R.W., Streckeisen, A., Zanettin, B., 1986. A chemical classification of volcanic rocks based on the total alkali–silica diagram. J. Petrol. 27, 745–750.
Lind, E.M., Wastegård, S., 2011. Tephra horizons contemporary with short early Holocene climate fluctuations: new results from the Faroe Islands. Quat. Int. 246, 157–167.
Long, A.J., Strzelecki, M.C., Lloyd, J.M., Bryant, C.L., 2012. Dating high Arctic Holocene relative sea level changes using juvenile articulated marine shells in raised beaches. Quat. Sci. Rev. 48, 61–66.
Lowe, D.J., 2011. Tephrochronology and its application: a review. Quat. Geochronol. 6 (3–4), 423.
Meara, R.H., Thordarson, T., Pearce, N.J.G., Hayward, C., Larsen, G., 2020. A catalogue of major and trace element data for Icelandic Holocene silicic tephra layers. J. Quat. Sci. 35, 122–142.

McCulloch, R.D., Figuerero Torres, M.J., Mengoni Goñalons, G., Barclay, R., Mansilla, C., 2017. A Holocene record of environmental change from Rio Zeballos, central Patagonia. Holocene 27 (7), 941–950.
Miller, G.H., Geirsdóttir, Á., Zhong, Y., Larsen, D.J., Otto-Bliesner, B.L., Holland, M.M., Bailey, D.A., Refsnider, K.A., Lehman, S.J., Southon, J.R., Anderson, C., Björnsson, H., Thordarson, T., 2012. Abrupt onset of the Little Ice Age triggered by volcanism and sustained by sea-ice/ocean feedbacks. Geophysical Research Letters 39 (2), L02708.
Muschitiello, F., Pausata, F.S.R., Lea, J.M., Mair, D.W.F., Wohlfarth, B., 2017. Enhanced ice sheet melting driven by volcanic eruptions during the last deglaciation. Nat. Commun. 8, 1020. https://doi.org/10.1038/s41467-017-01273-1.
Newton, A.J., 1999a. Ocean Transported Pumice in the North Atlantic. Doctoral thesis. University of Edinburgh, p. 394.
Newton, A.J., 1999b. Report on the pumice. In: Crawford, B.E., Ballin Smith, B. (Eds.), The Biggings, Papa Stour, Shetland: the History and Archaeology of a Royal Norwegian Farm. Society of Antiquaries of Scotland Monograph Series No 13, Edinburgh, p. 178.
Newton, A.J., 2000. Two fragments of pumice. In: Excavations at Dun Ardtreck, skye, in 1964 and 1965 (MacKie, E.). Proc. Soc. Antiq. Scotl. 130, 405–406.
Newton, A.J., 2001. The pumice. In: Mithen, S. (Ed.), Hunter Gather Landscape Archaeology: the Southern Hebrides Project 1988-98. McDonald Institute Monographs, Cambridge, pp. 403–405.
Newton, A.J., 2018. Pumice found at Udal. In: Ballin Smith, B. (Ed.), Life on the Edge: the Neolithic and Bronze Age of Iain Crawford's Udal, North Uist. Archaeopress, Oxford, pp. 165–168.
Noe-Nygaard, A., 1951. Sub-fossil Hekla pumice from Denmark. Medd. fra Dansk Geologisk Forening København 12, 36–46.
Nordenskiöld, A.E., 1863. Geografisk och geognostisk beskrifning öfer nordöstra delarne af Spetsbergen och Hinlopen Strait. K. Svenska Vet. Akad. Handl. Ny följd 4 (7), 1–25.
Norwegian Polar Institute, 2014. Terrengmodell svalbard (S0 Terrengmodell) [data set]. Norwegian Polar Institute. https://doi.org/10.21334/npolar.2014.dce53a47.
Óladóttir, B.A., Larsen, G., Thordarson, Th, Sigmarsson, O., 2005. The Katla volcano S Iceland, Holocene tephra stratigraphy and eruption frequency. Jokull 55, 53–74.
Óladóttir, B.A., Thordarson, Th, Larsen, G., Sigmarsson, O., 2007. Survival of the Mýrdalsjökull ice cap through the Holocene thermal maximum: evidence from sulphur contents in Katla tephra layers (Iceland) from the last ~8400 years. Ann. Glaciol. 45, 183–188.
Óladóttir, B.A., Sigmarsson, O., Larsen, G., Thordarson, Th, 2008. Katla volcano, Iceland, magma composition, dynamics and eruption frequency as recorded by tephra layers. Bull. Volcanol. 70, 475–493.
Óladóttir, B., Larsen, G., Guðmundsson, M.T., 2020. Katla. In: Oladottir, B., Larsen, G. & Guðmundsson, M. T. Catalogue of Icelandic Volcanoes. IMO, UI and CPD-NCIP. Retrieved from http://icelandicvolcanoes.is/?volcano=KAT. http://icelandicvolcanoes.is/?volcano=KAT.
Parry, W.E., 1828. Narrative for an Attempt to Reach the North Pole. J. Murray, London, p. 148.
Peulvast, J.P., Dejou, J., 1982. The occurrence of drift pumice on Holocene raised shorelines of the NE Atlantic - the petvik beach (vestvagpy, lofoten islands, north Norway). Comptes Rendus des Seances de L'Academie des Sciences Serie II - Mecanique Physique Chimie Sciences de L'Universe Sciences de La Terre 294, 405–408.
Ponomareva, V., Portnyagin, M., Davies, S.M., 2015. Tephra without borders: far-reaching clues into past explosive eruptions. Front. Earth Sci. 3, 83,. https://doi.org/10.3389/feart.2015.00083.
Romundset, A., Lakeman, T.R., Høgaas, F., 2018. Quantifying variable rates of post-glacial relative sea level fall from a cluster of 24 isolation basins in southern Norway. Quat. Sci. Rev. 197, 175–192.
Romundet, A., Lakeman, T.R., 2019. Shoreline displacement at Ørland since 6000 cal. yr. BP. In: Ystgaard, Ingrid (Ed.), Environment and Settlement: Ørland 600 BC - AD 1250: Archaeological Excavations at Vik, Ørland Main Air Base. Nordic Open Access Scholarly Publishing, Cappelen Damm Akademisk, Oslo, pp. 51–67.
Salvigsen, O., 1978. Holocene emergence and finds of pumice, whalebones, and driftwood at Svartknausflya, Nordaustlandet. Norsk Polarinstittot Årbok 1977, 217–228.
Salvigsen, O., 1981. Radiocarbon dated raised beaches in Kong Karls Land, Svalbard and their consequences for the glacial history of the Barents Sea area. Geogr. Ann. 63 (3–4), 283–291.
Salvigsen, O., 1984. Occurrence of pumice on raised beaches and the Holocene shoreline displacement in the inner Isfjorden area. Svalbard. Polar Research 2, 107–113.
Salvigsen, O., Österholm, H., 1982. Radiocarbon dated raised beaches and glacial history of the northern coast of Spitsbergen, Svalbard. Polar Res. 1, 97–115.
Schomacker, A., Krüger, J., Kjær, K.H., 2010. The Mýrdalsjökull ice cap, Iceland: glacial processes, sediments and landforms on an active volcano. In: Developments in Quaternary Science 13. Elsevier, Amsterdam, p. 211.
Schomacker, A., Farnsworth, W.R., Ingólfsson, Ó., Allaart, L., Håkansson, L., Retelle, M., Siggaard-Andersen, M.-L., Korsgaard, N.J., Rouillard, A., Kjellman, S.E., 2019. Postglacial relative sea level change and glacier activity in the early and late Holocene: Wahlenbergfjorden, Nordaustlandet, Svalbard. Sci. Rep. 9, 6799.
Schmid, R., 1981. Descriptive nomenclature and classification of pyroclastic deposits and fragments: recommendations of the IUGS Subcommission on the Systematics of Igneous Rocks. Geology 9, 41–43.
Schytt, V., Hoppe, G., Blake, W., Grosswald, M.G., 1968. The extent of the würm glaciation in the European arctic. International Association of Scientific Hydrology 79, 207–216.
Sessford, E.G., Strzelecki, M.C., Hormes, A., 2015. Reconstruction of past patterns of change in a High Arctic coastal landscape, southern Sassenfjorden, Svalbard. Geomorphology 234, 98–107.
Strøm, H., 1762. Physisk og oeconomisk beskrivelse over Fogderiet søndmør. Beliggende i Bergens Stift, i Norge 2, 1762–1766. Sorøe.
Smith, K.T., Dugmore, A.J., 2006. Jökulhlaups circa landnám: mid- to late first millennium AD floods in south Iceland and their implications for landscapes of settlement. Geografiske Annaler 88 (2), 165–176.
Striberger, J., Björck, S., Holmgren, S., Hamerlík, L., 2012. The sediments of Lake Lögurinn e a unique proxy record of Holocene glacier meltwater variability in eastern Iceland. Quat. Sci. Rev. 38, 76–88.
Stötter, J., Wastl, M., Caseldine, C., Haberle, T., 1999. Holocene palaeoclimatic reconstructions in northern Iceland: approaches and results. Quat. Sci. Rev. 18, 457–474.
Thorarinsson, S., 1944. Tefrokronologiska studier på Island. (Tephrochronological studies in Iceland). Geogr. Ann. 26, 395–398.
Thorarinsson, S., 1974. The terms tephra and tephrochronology. In: Westgate, J.A., Gold, C.M. (Eds.), World Bibliography and Index of Quaternary Tephrochronology. INQUA/UNESCO, Edmonton, Alberta, pp. 17–19.
Thorsteinsdóttir, E.S., Guðmundsdóttir, E.R., Larsen, G., 2015. Grain characteristics of tephra from the subglacial SILK-LN Katla eruption 3400 years ago and the subaerial Hekla eruption in 1947. Jokull 65, 29–49.
Thorsteinsdóttir, E., Larsen, G., Guðmundsdóttir, E.R., 2016. Grain characteristics of silicic Katla tephra layers indicate a fairly stable eruption environment between 2800 and 8100 years ago. Jokull 62, 69–81.
Timms, R.G.O., Matthews, I.P., Lowe, J.J., Palmer, A.P., Weston, D.J., MacLeod, A., Blockley, S.P.E., 2019. Establishing tephrostratigraphic frameworks to aid the study of abrupt climatic and glacial transitions: a case study of the Last Glacial-Interglacial Transition in the British Isles (c. 16-8 ka BP). Earth Sci. Rev. 192, 34–64.
Tómasson, H., 1996. The jökulhlaup from Katla in 1918. Ann. Glaciol. 22, 249–254.
Undas, I., 1942. On the late-Quaternary history of Møre and Trøndelag (Norway). Det KGL Norske Videnskabers Selskabs Skrifter 2, 1–92.
Valdimarsson, H., Malmberg, S.-A., 1999. Near-surface circulation in Icelandic waters derived from satellite tracked drifters. Rit Fiskid. 16, 23–39.
van der Bilt, W.G.M., Lane, C.S., Bakke, J., 2017. Ultra-distal Kamchatkan ash on Arctic Svalbard: towards hemispheric cryptotephra correlation. Quat. Sci. Rev. 164, 230–235.
Wastegård, S., 2002. Early to middle Holocene silicic tephra horizons from the Katla volcanic system, Iceland: new results from the Faroe Islands. J. Quat. Sci. 17, 723–730.
Wastegård, S., Davies, S., 2009. An overview of distal tephrochronology in northern Europe during the last 1000 years. J. Quat. Sci. 24, 500–512.
Wastegård, S., Guðmundsdóttir, E.R., Lind, E.M., Timms, R.G.O., Björck, S., Hannon, G.E., Olsen, J., Rundgren, M., 2018. Towards a Holocene tephrochronology for the Faroe Islands, north Atlantic. Quat. Sci. Rev. 195–214.
Whitham, A.G., Sparks, R.S.J., 1986. Pumice. Bull. Volcanol. 48, 209–223.
Zamelczyk, K., Rasmussen, T.L., Husum, K., Haflidason, H., de Vernal, A., Ravna, E.K., Hald, M., Hillaire-Marcel, C., 2012. Paleoceanographic changes and calcium carbonate dissolution in the central Fram Strait during the last 20 ka yr. Quat. Res. 78, 405–416.